Advances in Engineering Research : Possibilities and Challenges
ISSN Print: 3079-5192
ISSN Online: 3079-5206
https://doi.org/10.63313/AERpc.9038

Dynamic mesh stiffness of spur gear using transient dynamic analysis

Yueyao Xiao. Fuhao Liu
School of Mechanical and Automotive, Qingdao University of Technology, Qingdao 266520, China
Email: 2183059844@qq.com

How to cite this paper: Xiao, Y. Y., & Liu, F. H. (2025). Dynamic mesh stiffness of spur gear using transient dynamic analysis. Advances in Engineering Research: Possibilities and Challenges, 2(1), 66-73. ISSN Print: 3079-5192; ISSN Online: 3079-5206. https://doi.org/10.63313/AERpc.9038
Published: 2025-07-24

Abstract

Due to model and computational constraints, traditional gear rotor system analyses often oversimplify dynamic mesh stiffness (DMS) variations and in-stead rely on static mesh stiffness (SMS) assumptions. This simplification ig-nores the speed-dependent stiffness fluctuations that are critical to the gear meshing system. In order to calculate the dynamic meshing stiffness of gears dependent on velocity, a spur gear model based on Euler beams is proposed, and the transient dynamics method (TDA) is adopted. The calculation methods are validated by both software. The results show that there is a significant change in the dynamic meshing force with respect to the velocity, which provides support for further research on gear rotor dynamics.

Keywords

Dynamic mesh stiffness (DMS); spur gear model; transient dynamics method (TDA)

1. Introduction

Gear transmissions are critical mechanical components found in a wide range of machinery. The industrial applications are countless and cover fields such as aerospace, agriculture or wind generation among others. As the working speeds for gear transmissions increase [1], the dynamic problems become more important. The main feature that characterizes dynamic behavior is the periodic excitation induced by the variable meshing stiffness [2]. Especially in spur gears, where the magnitude of transmission speed changes the characteristics of mesh stiffness, thereby altering dynamic behavior. To achieve better analysis [3], improve durability, and reduce noise and vibration levels during the design phase, accurate estimation and calculation of meshing stiffness have become the key to solving gear dynamics problems.

In gear system dynamics studies, meshing stiffness is an important excitation for the vibration of nonlinear systems. However, ensuring the accuracy of mesh stiffness and its applicability in gear dynamics is still a challenging problem and attracts extensive attention. Zhang et al. [4] integrated the advantages of Hertzian contact theory, FEM and slice approach to calculating the mesh stiffness. Xu et al. [5] established a mesh stiffness model for planetary gear considering the position-dependent Hertzian contact deformation. However, recent studies have shown that SMS cannot accurately represent the mesh stiffness of gear pairs. The mesh stiffness should be calculated by taking dynamic conditions into account to adapt to the actual conditions. Therefore, Cao et al. [6] established a force-dependent mesh stiffness model considering the effect of force-dependent time-varying mesh stiffness, backlash, and profile deviation. Jiang et al. [7] calculated the mesh stiffness based on the energy method by incorporating the integration of speed to obtain instantaneous angular displacement. However, the above mesh stiffness studies are carried out under a static framework. Although Xie and Yu [8] conducted pioneering investigations on gear meshing stiffness, their computational outcomes predominantly reflect static stiffness characteristics rather than dynamic behaviors. Furthermore, Shi and Li [9] introduced a dynamic meshing stiffness model incorporating time-varying meshing forces specific to hypoid gears. Despite the above progress, there is still a lack of beam element-based tooth modeling to explore the effect of travel speed on mesh stiffness.

Based on transient dynamics, new calculations are proposed to calculate DMS by treating teeth as variable section cantilever beams, where the relationship is established between the meshing force and the meshing displacement. The content of this article is summarized as follows. Section 2 explains the establishment of an improved wheel tooth model. In section 3, the validity of the model is verified with the natural frequencies of both software. Section 4 analyzes the trend and fluctuation of static and dynamic meshing stiffness under different methods.

2. Spur gear system dynamic modeling

2.1. Model of variable center distance of gears

The dynamic mesh stiffness of the gear refers to the mesh stiffness of the mesh gear teeth under working conditions. The actual mesh state of the gear pair is different from the static state, which varies with the driving speed. Thus, the dynamic mesh stiffness of the gear must be determined according to the driving speed. In this section, based on e ISO standard 6336 and Euler Bernoulli beam theory, the transient dynamics analysis (TDA) will be used to solve the dynamic displacement of gear teeth, to get dynamic meshing stiffness.

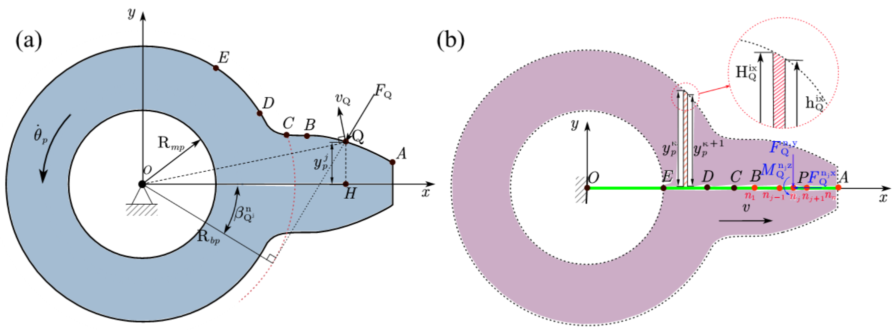

Figure 1. Analytical model of the stiffness calculation of gear (a)The model of gear tooth, (b)The model of Euler-Bernoulli beam

2.2. Calculation of gear tooth dynamic displacement

The gear model could be simplified as a cantilever Euler beam, as shown in Fig. 1(b). $F_Q^{n_j x}$ and $F_Q^{n_j y}$ are the components of mesh force in the x and y directions, respectively. $M_Q^{n_j z}$ denotes torque of the mesh point. These parameters can be expressed as:

$$F_Q^{n_j x} = F_Q \sin\left(\beta_Q^{n_j}\right), \quad F_Q^{n_j y} = F_Q \sin\left(\beta_Q^{n_j}\right), \quad M_Q^{n_j z} = F_Q \sin\left(\beta_Q^{n_j}\right) y_Q^{n_j} \tag{1}$$

here, $\beta_Q^{n_j}$ is the mesh angle of gear tooth at any position on the mesh line. And according to the gear mesh principle, it can be expressed as:

$$\beta_Q^{n_j} = \arccos\left(R_{bp} \Big/ \sqrt{\left(x_Q^{n_j}\right)^2 + \left(y_Q^{n_j}\right)^2} \right) - \arctan\left(y_Q^{n_j} \big/ x_Q^{n_j} \right) \tag{2}$$

here, $x_Q^{n_j}$ and $y_Q^{n_j}$ denote the x and y coordinate of the mesh point, respectively. The DMS of the tooth could be obtained according to the bending deflection change of the Euler beam in the mesh process. And the dynamic calculate equation for DMS can be written as:

$$M\ddot{X}_Q + C\dot{X}_Q + KX_Q = F_Q\left(\dot{\theta}_p\right) \tag{3}$$

here, M, C, and K are the matrix of global mass, damping, and stiffness of pinion, respectively. The matrix of global can be calculated as:

$$M = \sum_{i=1}^{N}\left[M_Q^{ix}\right], \quad K = \sum_{i=1}^{N}\left[K_Q^{ix}\right], \quad C = \sum_{i=1}^{N}\left\{\alpha_M\left[M_Q^{ix}\right] + \beta_K\left[K_Q^{ix}\right]\right\} \tag{4}$$

The X_Q are represents the total displacement matrix of the mesh point, which can be expressed as follows:

$$X_Q = \left[X_Q^{n_1} \quad \cdots \quad X_Q^{n_j-1} \quad X_Q^{n_j} \quad X_Q^{n_j+1} \quad \cdots \quad X_Q^{n_n} \right]^T \tag{5}$$

here, $X_Q^{n_j}$ are represent the displacement matrix of the mesh point. It can be expressed as follows:

$$X_Q^{n_j} = \left[\Delta x_Q^{n_j} \quad \Delta y_Q^{n_j} \quad \Delta \theta_Q^{n_j z} \right]^T \tag{6}$$

here, $\Delta x_Q^{n_j}$, $\Delta y_Q^{n_j}$ and $\Delta \theta_Q^{n_j}$ are the elastic deformation of mesh point in the x, y and θ directions, respectively.

The elastic deflection of the beam from the previous moment of mesh affects the state of mesh at the subsequent moment. Hence, the acceleration $\ddot{X}_Q$, velocity $\dot{X}_Q$ and displacement X_Q at mesh point can be calculated as:

$$\ddot{X}_Q^{n_j+1} = a_0\left(X_Q^{n_j+1} - X_Q^{n_j} \right) - a_2 \dot{X}_Q^{n_j} - a_3 \ddot{X}_Q^{n_j} \tag{7}$$

$$\dot{X}_Q^{n_j+1} = a_1\left(X_Q^{n_j+1} - X_Q^{n_j} \right) - a_4 \dot{X}_Q^{n_j} - a_5 \ddot{X}_Q^{n_j} \tag{8}$$

$$\begin{aligned}\left(a_0 M + a_1 C + K \right) X_Q^{n_j+1} = F_Q^{n_j+1} + M\left(a_0 X_Q^{n_j} + a_2 \dot{X}_Q^{n_j} + a_3 \ddot{X}_Q^{n_j} \right) \\ + C\left(a_1 X_Q^{n_j} + a_4 \dot{X}_Q^{n_j} + a_5 \ddot{X}_Q^{n_j} \right)\end{aligned} \tag{9}$$

here, $a_0 = 1/\left(\alpha \cdot (\Delta t_p^{n_j})^2\right)$, $a_1 = \delta/\left(\alpha \cdot \Delta t_p^{n_j}\right)$, $a_2 = 1/\left(\alpha \cdot \Delta t_p^{n_j}\right)$, $a_3 = 1/2\alpha - 1$, $a_4 = \delta/\alpha - 1$, $a_5 = \Delta t_p^{n_j} \cdot (\delta/\alpha - 2)/2$. The α and δ are calculate in research[10] and the time step between the mesh force moving from the front mesh point to the rear mesh point, which can be expressed by the mesh speed as:

$$\Delta t_Q^{n_j} = 2\sqrt{\left(\Delta x_Q^{n_j} \right)^2 + \left(\Delta y_Q^{n_j} \right)^2} \Big/ \left(v_Q^{n_j} + v_Q^{n_j-1} \right) \tag{10}$$

here, the mesh speed can be expressed by the driving speed as:

$$v_Q^{n_j} = \dot{\theta}_p \sqrt{\left(\left(x_Q^{n_j} \right)^2 + \left(y_Q^{n_j} \right)^2 \right)} \tag{11}$$

Then, the total dynamic displacement of gear tooth for the mesh point n_j can be calculated as:

$$\Delta \delta^{n_j}\left(\dot{\theta}_p \right) = \sqrt{\left(\Delta x_Q^{n_j} \right)^2 + \left(\Delta y_Q^{n_j} \right)^2} \cos\left(\arctan\left(x_Q^{n_j} / y_Q^{n_j} \right) - \beta_Q^{n_j} \right) \tag{12}$$

Through the above deduce, the DMS of pinion and gear for the mesh point n_j can be obtained as:

$$k_{p,g}^{n_j}\left(\dot{\theta}_p\right)=\frac{F_Q^{n_j}}{\Delta\delta^{n_j}\left(\dot{\theta}_p\right)} \tag{13}$$

In one mesh cycle of the gear, there will be a single-tooth mesh region and a double-tooth mesh region. When the two teeth mesh at the same time, which can be seen as a series connection of DMS of the two pairs of teeth. Hence, the DMS for one mesh cycle can be calculated as:

$$k_{md}\left(\dot{\theta}_p\right)=k_m^1\left(\dot{\theta}_p,\dot{\theta}_g\right)+k_m^2\left(\dot{\theta}_p,\dot{\theta}_g\right) \tag{14}$$

3. Gear stiffness comparison and verification

Table 1. Gear parameters.

Parameters	Pinion (driving gear)	Gear (driven gear)
Teeth number	23	31
Module (mm)	2.5	
Teeth width (mm)	20	
Contact ratio	1.6262	
Pressure angle (°)	20	
Poisson's ratio	0.3	
Young's modulus E (Pa)	206E9	
Gear mesh damping ratio	0.025	
Bearing damping ratio	0.075	

In the dynamic condition, the actual mesh state of the gear pair is different from the static condition, and it varies with the driving speed. MSM is mainly used to solve the dynamic mesh stiffness of the spur gears in this study. In this section, static meshing stiffness and dynamic meshing stiffness are compared using the proposed method, Full method in transient dynamic analysis, potential energy method [11] and finite element method. The gear parameters used in this paper are listed in Table 1.

Table 2. Natural frequencies of pinion teeth and gear teeth (Hz).

Mode	Pinion		Error(%)	Gear		Error(%)
	Ansys	Fortran		Ansys	Fortran	
1	41517	41927	0.99	30247	30602	1.17
2	52595	52744	0.28	38216	38323	0.28
3	130639	132022	1.06	98634	102314	3.73
4	141736	145359	2.56	113930	114201	0.24
5	164778	155124	0.22	140659	141856	0.85
6	223668	224065	0.18	184663	184835	0.09
7	261817	265827	1.53	187504	191561	2.16
8	280616	281505	0.32	228436	228770	0.15

In Table 2, the modal analysis of the large and small gears of the cantilever beam with the equivalent variable cross-section is carried out by the two software, and the first eight natural frequencies and the relative differences between the frequencies $(\boldsymbol{\omega}/2\boldsymbol{\pi})$ of the two software are solved. It can be observed that the errors of the first eight natural frequencies are all within 4%.

4. Results and discussion

Fig. 2(a) is a comparison of the static stiffness of TDA and PEM for Fortran and Ansys. According to the Euler-Bernoulli beam theory [12], the static stiffness of the TDA is obtained by applying a meshing force to the gear teeth under quasi-static conditions (n_p = 0.01 rpm). As can be seen from the graph, the static stiffness curves of Fortran and Ansys' TDA are relatively close, and there are some errors in the results of the PEM and the other two methods compared to the results of the PEM calculations. It is important to note that PEM cannot consider the effects of speed.

Fig. 2(b) shows a comparison of the dynamic stiffness of the TDA from Fortran and Ansys. The driving speed of the pinion is n_p = 300 rpm. As can be seen from the graph, the dynamic stiffness of the gear fluctuates around the quasi-static stiffness when the gear begins to mesh. The closer the meshing position is to the root, the greater the range of fluctuations in tooth stiffness. This is caused by a change in the damping and meshing forces perpendicular to the centerline of the gear teeth. Because the meshing point is closer to the tooth root, the greater the component of the meshing force perpendicular to the tooth centerline, resulting in a large fluctuation of the tooth dynamic stiffness. The near-complete overlap between Ansys and Fortran's TDA methods validates the accuracy of these methods.

As shown in Fig. 3(a), it can be observed that the driving speed has no effect on static stiffness. Nevertheless, in Fig. 3(b), due to the resonance effect of periodic meshing impact on the system, the comprehensive grid stiffness will fluctuate. It is worth mentioning that the resonance peak appears skewed rather than shifted, which is the result of the meshing frequency modulation affecting the meshing from the frequency domain to the high frequency band.

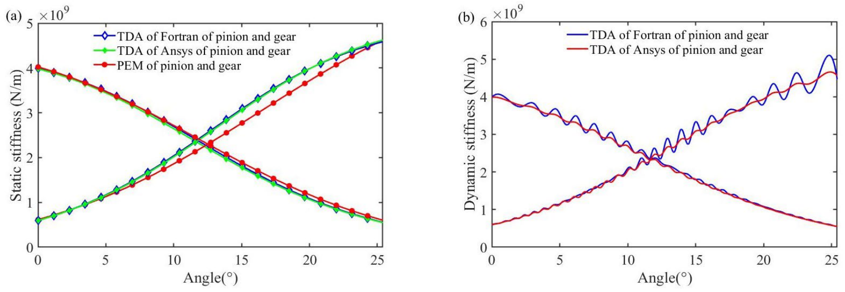

Figure 2. Comparison of static stiffness and dynamic stiffness of a single gear tooth (a) Static stiffness, (b) Dynamic stiffness.

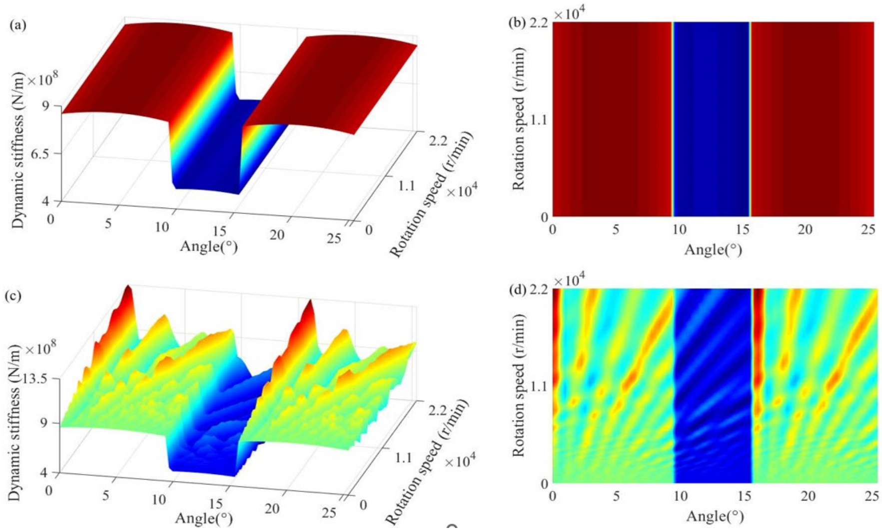

Figure 3. Influence of driving speed on the dynamic mesh stiffness of comprehensive mesh stiffness (a) SMS (b) contour map (c) DMS (d) contour map

5. Conclusion

In this paper, a gear tooth model based on Euler beams is established, and the dynamic stiffness (DMS) of velocity-affected meshing is derived by transient dynamics (TDA). The accuracy of the model was verified with two software, and the accuracy of the initial 8 natural frequencies of the gear teeth fell within 4%. The meshing dynamic stiffness (DMS) determined by the Transient Dynamics Method (TDA) is accurate up to 0.3% with tolerable inaccuracies. In the 3D diagram, due to the influence of meshing frequency modulation, the resonant peak is skewed to the right instead of translated.

References

[1] B. Hu, C. Zhou, H. Wang, S. Chen, (2021) Nonlinear tribo-dynamic model and experimental verification of a spur gear drive under loss-of-lubrication condition, Mechanical Systems and Signal Processing 153,107509.

[2] H.N. Özgüven, D.R. Houser, (1988) Mathematical models used in gear dynamics—a review, Journal of Sound and Vibration 121, 383–411.

[3] F. Oyague, (2009) Gearbox Modeling and Load Simulation of a Baseline 750-kW Wind Turbine Using State-of-the-Art Simulation Codes. NREL/TP-500-41160 February 2009.

[4] C. Zhang, H. Dong, D. Wang, B. Dong, (2022) A new effective mesh stiffness calculation method with accurate contact deformation model for spur and helical gear pairs, Mechanism and Machine Theory 171, 104762.

[5] Z. Xu, W. Yu, Y. Shao, X. Yang, C. Nie, D. Peng, (2022) Dynamic modeling of the planetary gear set considering the effects of positioning errors on the mesh position and the corner contact, Nonlinear Dynamics 109 (3) 1551–1569.

[6] H. Han, S. Zhang, Y. Yang, H. Ma, L. Jiang, (2022) Modulation sidebands analysis of coupled bevel gear pair and planetary gear train system, Mechanism and Machine Theory 176, 104979.

[7] F. Jiang, Y. Zhu, W. K. Ding, (2024) Vibration modulation features analysis of fixed-shaft gear train considering speed fluctuation and flexible transmission path based on signal convolution model, Mechanical Systems and Signal Processing 211 (Apr.) 111250.

[8] C. Xie, W. Yu, (2022) Gear dynamic modelling based on the concept of dynamic mesh stiffness: theoretical study and experimental verification, Journal of Mechanical Science and Technology 36, 4953–4965.

[9] Z. Shi, S. Li, (2022) Nonlinear dynamics of hypoid gear with coupled dynamic mesh stiffness, Mechanism and Machine Theory 168, 104589.

[10] F. Liu, H. Jiang, S. Liu, X. Yu, (2016) Dynamic behavior analysis of spur gears with constant and variable excitations considering sliding friction inffuence, Journal of Mechanical Science and Technology 30, 5363–5370.

[11] H. Jiang and F. Liu, (2019) Analytical models of mesh stiffness for cracked spur gears considering gear body deflection and dynamic simulation, Meccanica, vol. 54, no. 11, pp. 1889-1909.

[12] E. Carrera, G. Giunta, and M. Petrolo, (2011) beam structures (classical and advanced theories) || the Euler Bernoulli and timoshenko theories, vol. 10.1002/9781119978565, pp. 169-180.